

Band Structure of Silicon from an Adjusted Heine-Abarenkov Calculation

E. O. KANE

Bell Telephone Laboratories, Murray Hill, New Jersey

(Received 7 January 1966)

The band structure of silicon has been computed using the Heine-Abarenkov pseudopotential method. The theoretical Fourier coefficients of the potential were then varied on the order of 30% to give agreement with measured cyclotron masses and the indirect gap. The resultant band structure is close to that obtained by Brust, Cohen, and Phillips using only the three lowest potential coefficients. We find that the higher potential coefficients are not weak but are nearly linearly dependent in their effect on the band-structure parameters investigated. The distribution in k space of contributions to $\epsilon_2(\omega)$ was studied and found to be poorly described by contributions from the symmetry points at Γ , X , and L . Nevertheless, the optical gaps at Γ , X , and L are fairly close in energy to the three prominent peaks, 3.5, 4.3, and 5.4 eV in $\epsilon_2(\omega)$. For the 4.3-eV peak, at least, this proximity in energy is found to be relatively insensitive to variations in the potential which maintain cubic symmetry.

I. INTRODUCTION AND CONCLUSIONS

THE pseudopotential method¹⁻³ has permitted the characterization of crystal potentials in terms of a very small number of parameters, the Fourier coefficients of the potential, $V(K)$, for the K vectors of the reciprocal lattice. The number of parameters is determined by how many "different" plane waves (waves inequivalent under the symmetry operations of the lattice) interact strongly with the free-electron basis states. The reduction of the band-structure problem to a small number of parameters allows one to determine these parameters empirically as soon as one can measure a few experimental quantities closely related to band structure. Phillips¹ was the first to note that a "reasonable" band structure for silicon could be obtained with the use of only two parameters. A third parameter was later added as a refinement.

In metals the pseudopotential parameters have been determined by fairly unambiguous Fermi-surface measurements.³ In silicon, germanium, and other semiconductors the main emphasis has been on fitting the band structure to reproduce the fundamental optical absorption.

It is generally believed that structure in $\epsilon_2(\omega)$, the imaginary part of the dielectric constant, is due to critical points⁴ in the optical energy bands, $E_c(\mathbf{k}) - E_v(\mathbf{k})$, where c and v refer to conduction and valence bands, respectively. A critical point is defined as a point where $\nabla_{\mathbf{k}}(E_c(\mathbf{k}) - E_v(\mathbf{k})) = 0$. Critical points are required by symmetry at Γ and L in the diamond lattice but may also occur at points of lower symmetry.

In the interpretation of optical-absorption spectra it has been common practice to associate critical-point structure with high-symmetry points.^{5,6} The most

recent empirical band structure of silicon and germanium, that of Brust, Cohen, and Phillips,⁵ was determined on the basis of this assumption. We shall refer to this work as the BCP band structure. The three peaks in the optical absorption spectra were used to determine the three lowest pseudopotential coefficients, $V([\frac{2\pi}{a}](1,1,1))$, $V([\frac{2\pi}{a}](2,2,0))$, and $V([\frac{2\pi}{a}] \times (3,1,1))$. All other coefficients were taken to be zero. A local (k -independent) potential was assumed.

We have undertaken to re-examine this problem because we felt that a number of the above assumptions were questionable.

Our approach has been to do as good a "first principles" calculation as possible without an undue amount of labor and then to adjust the *a priori* potential by as little as possible to fit those experimental band structure parameters which are most reliably established, namely, the cyclotron masses in the valence and conduction band and the indirect band gap. We have chosen the Heine-Abarenkov⁷ pseudopotential method as the best, simple "first principles" model. This we describe in Sec. II.

On the basis of our calculation we have then tested the assumptions made by Brust, Cohen, and Phillips⁵ for silicon. We find that, although their assumptions were rather poor, their band structure is very close to ours. This seems to be attributable to the fact that the silicon band structure is, indeed, characterizable by a very small number of parameters.

We have found that optical-energy critical point structure in silicon cannot be accurately attributed to regions near Γ , X , and L but instead comes from very large regions in k space where the optical energy surface is nearly k -independent. These regions are apparently due to several critical points of nearly equal energy.

Even though the symmetry critical points make only a small contribution to the optical-critical-point structure, it is true that the optical gap at the symmetry

¹ J. C. Phillips, Phys. Rev. **112**, 685 (1958).

² J. C. Phillips and L. Kleinman, Phys. Rev. **116**, 287 (1959); M. H. Cohen and V. Heine, *ibid.* **122**, 1821 (1961); B. J. Austin, V. Heine, and L. J. Sham, *ibid.* **127**, 276 (1962).

³ W. A. Harrison, Phys. Rev. **126**, 497 (1962); N. W. Ashcroft, Phil. Mag. **8**, 2055 (1963).

⁴ J. C. Phillips, J. Phys. Chem. Solids **12**, 208 (1960).

⁵ D. Brust, M. L. Cohen, and J. C. Phillips, Phys. Rev. Letters **9**, 389 (1962).

⁶ H. Ehrenreich, H. R. Philipp, and J. C. Phillips, Phys. Rev.

Letters **8**, 59 (1962); J. C. Phillips, Phys. Rev. **133**, A452 (1964); M. Cardona and G. Harbeke, J. Appl. Phys. **34**, 813 (1963); M. Cardona and D. L. Greenaway, Phys. Rev. **131**, 98 (1963).

⁷ V. Heine and I. Abarenkov, Phil. Mag. **9**, 451 (1964).

points is close in energy to the absorption peaks with which they have been associated.

We have studied the k distribution of the 4.3-eV peak in most detail. This is the largest of the experimental peaks and we find that it originates from the largest region in k space. The X point is on the edge of this large region. We have tested the "stability" of this large region to variations of the potential and find that to within $\sim 20\%$ the region tends to shift in energy as a whole. The resulting peak then moves in energy as the potential is varied but does not broaden rapidly. The X point is 0.2 eV lower than the main peak, but it also shifts with the main peak.

A pseudopotential is inherently angular momentum-dependent because "s" functions sample more of the core than p or d electrons. This results in a k -dependent or nonlocal potential. We have included this k dependence and find that it contributes $\sim 10\%$ to the cyclotron masses. The empirical potential of Brust, Cohen, and Phillips⁵ was k -independent but, again, this has not led to significant discrepancies between our resulting band structures.

Exchange also makes a k -dependent contribution to the potential, in principle, at least. We have computed the exchange potential for free electrons at the density of silicon using dynamically screened exchange as calculated by Quinn and Ferrell.⁸ We find that the exchange energy varies by less than 0.03 eV between the Fermi energy, E_F , and E_F+7 eV. It appears that exchange will primarily act to shift the bands as a whole, so we have not included it in our calculation.

The Heine-Abarenkov potential gives considerable importance to the high plane wave components of the pseudopotential. This might seem to invalidate the three parameter approach of Brust, Cohen, and Phillips.⁵ We find that the BCP band structure is good, not because the high Fourier coefficients of the potential are unimportant, but because they are not linearly independent in their effects on the band structure constants which we have tested.

The largest discrepancy between the BCP band structure and our own is the $\Gamma_{25'}-\Gamma_{2'}$ separation which we find to be 3.3, or 0.5 eV lower than BCP.

II. HEINE-ABARENKOV MODEL POTENTIAL

We have chosen the Heine-Abarenkov⁷ method as the simplest way to obtain a reasonable zeroth approximation to the silicon band structure. We then adjust the potential obtained in this manner in order to fit the well-established indirect energy-gap and cyclotron-resonance masses.

Following Heine and Abarenkov,⁷ we calculate an angular momentum-dependent (nonlocal) potential for the bare ions which we then screen by a k -dependent dielectric constant as calculated for a free-electron gas

⁸ J. J. Quinn and R. A. Ferrell, Phys. Rev. **112**, 812 (1958).

TABLE I. Effective square-well depths which reproduce the atomic levels of Si^{3+} ; $1.15a_0$ well radius. Potential energy given by $-4e^2/r$ outside square well.

l	Atomic level binding energy in rydbergs	Effective square-well depth in rydbergs	
0	-3.32	-1.74	
0	-1.55	-1.46	
0	-0.59	-1.22	
1	-2.66	-3.37	
1	-1.33	-3.59	
1	-0.53	-3.67	
2	-1.86	-10.3	
2	-1.04	-10.4	
2	-0.46	-10.5	
0	-2.3	-1.59	Interpolated
1	-2.3	-3.43	
2	-2.3	-10.3	

of the same average density as the valence charge density of silicon (4 electrons per atom).

The bare ion potential is represented as a superposition of contributions from each individual ion. The single ion potential is approximated by a square-well core and a Coulomb potential with $Z=4$ outside the core. The radius of the square well core was arbitrarily taken as $1.15 a_0$ (Bohr radii). The depth of the core was taken to be l -dependent and was determined to reproduce the free-ion energy levels of Si^{3+} .

The effective square-well depths for Si^{3+} are shown in Table I. The depths are seen to be strongly l -dependent. Although the energy dependence is much weaker, it is not negligible, especially for $l=0$ states. We have not included the energy dependence of the square-well parameters in our calculation but have instead evaluated them at a fixed energy which we think is a reasonable average value for the bands of greatest interest.

The valence electron-core interaction is chiefly governed by the energy difference between the valence electrons and the core electrons. Donley⁹ has obtained a value of 6.97 Ry for the $3s-2p$ separation in Si^{3+} using a Hartree calculation. Herman and Skillman¹⁰ find a $3s-2p$ separation of 6.96 Ry for the neutral silicon atom using a Hartree calculation with a "free-electron" exchange potential. Although the $3s$ level in Si^{3+} and Si differs by 2.3 Ry, the $3s-2p$ splitting is independent of this large shift to within the accuracy of the calculations. We assume that this also holds true for the $3s-2p$ separation in the crystal. We are primarily interested in the energy region around the valence band maximum which lies approximately 1 Ry above the crystalline s state (lowest Γ_1 valence band at $k=0$). Hence, we evaluate the pseudopotential coefficients at 1 Ry above the $3s$ state in Si^{3+} , namely at -2.3 Ry. The interpolated square-well depths at this energy are shown in Table I.

⁹ H. L. Donley, Phys. Rev. **50**, 1012 (1936).

¹⁰ F. Herman and S. Skillman, *Atomic Structure Calculations* (Prentice-Hall, Inc., Englewood Cliffs, New Jersey, 1963).

TABLE II. k -dependent pseudopotential Fourier coefficients, $V_F(\mathbf{k}_1, \mathbf{k}_2)$. The numbers in parentheses in the right-hand column are the values of k_1^2 and k_2^2 in units of $(2\pi/a)^2$; they are followed by the energy, $V_F(\mathbf{k}_1, \mathbf{k}_2)$ in Ry. $\mathbf{K} = \mathbf{k}_1 - \mathbf{k}_2$. $F(K)$ are the factors required to adjust the Heine-Abarenkov potential to give cyclotron masses and an indirect energy gap agreeing with experiment. ϵ_{Lind} is the Lindhard dielectric constant. ϵ_{Hub} is the Lindhard dielectric constant with the Hubbard exchange correction.

K in units of $2\pi/a$	$F(K)$	$\epsilon_{\text{Lind}}(K)$	$\epsilon_{\text{Hub}}(K)$	$V_F(k, k')$ (in Ry)
(0,0,0)	1	1	1	(0.722, 0.722)0.004 (1.322, 1.322)0.000 (2.022, 2.022)-0.008 (3,3)-0.018 (4,4)-0.028
(1,1,1)	1.29	1.97	1.76	(0.722, 2.022)-0.213 (1.322, 2.022)-0.214 (3,4)-0.224
(2,2,0)	0.71	1.26	1.18	(2.022, 2.022)0.0385 (3,3)0.0370 (4,4)0.0352
(3,1,1)	0.71	1.12	1.07	(3,4)0.0640
(2,2,2)	0.086	1.09	1.06	(3,3)0.0082
(4,0,0)	1.02	1.05	1.03	(4,4)0.101
$K^2 \geq 19$	0.58			

Following Heine and Abarenkov,⁷ we construct an ionic potential, $V_{3+}(r, r')$ by taking a lattice sum over the individual ionic potentials, $v_{3+}(r - \mathbf{R}_i, r' - \mathbf{R}_i)$

$$V_{3+}(r, r') = \sum_{\mathbf{R}_i} v_{3+}(r - \mathbf{R}_i, r' - \mathbf{R}_i). \quad (1)$$

We have to use a nonlocal potential, $v(r, r')$ or $v(k, k')$, because our model potential is angular momentum-dependent. The sum is over lattice sites, \mathbf{R}_i . The lattice sum is easily performed in k space:

$$V_{3+}(r, r') = \sum_{\mathbf{k}, \mathbf{K}} \frac{N}{V} \cos(\mathbf{K} \cdot \boldsymbol{\tau}/2) v_{3+}(\mathbf{k}, \mathbf{k}') e^{i\mathbf{k} \cdot r} e^{-i\mathbf{k}' \cdot r'},$$

$$\mathbf{K} = \mathbf{k} - \mathbf{k}', \quad (2)$$

$$v_{3+}(\mathbf{k}, \mathbf{k}') \equiv \int e^{-i\mathbf{k} \cdot r} v_{3+}(r, r') e^{i\mathbf{k}' \cdot r'} dx dr',$$

where \mathbf{K} is a principal vector of the reciprocal lattice. The origin is taken midway between two nearest neighbors so that matrix elements will be real. N/V is the number of atoms per unit volume. The valence electrons are taken into account by screening the ionic potential with a k -dependent dielectric constant, $\epsilon_{\text{Hub}}(K)$

$$V_{\text{HA}}(\mathbf{k}, \mathbf{k}') = \frac{N}{V} v_{3+}(\mathbf{k}, \mathbf{k}') / \epsilon_{\text{Hub}}(K),$$

$$V_{\text{HA}}(r, r') = \sum_{\mathbf{k}, \mathbf{K}} V_{\text{HA}}(\mathbf{k}, \mathbf{k}') \cos \frac{\mathbf{K} \cdot \boldsymbol{\tau}}{2} e^{i\mathbf{k} \cdot r} e^{-i\mathbf{k}' \cdot r'}. \quad (3)$$

The dielectric constant ϵ_{Lind} , is evaluated in the free-electron self-consistent-field approximation¹¹ (Lindhard dielectric constant) using an electron density equal to 4 electrons per silicon atom. The Hubbard exchange correction is then added with the formula⁷

$$\epsilon_{\text{Hub}}(K) = (\epsilon_{\text{Lind}} - 1) \times \{1 - [K^2/2(K^2 + k_F^2 + (2k_F/\pi a_0))] + 1\}, \quad (4)$$

where k_F is the Fermi momentum. Penn¹² has shown that the free-electron approximation is not too bad for the dielectric constant of an insulator for large k vectors. Since the principal lattice vectors are of the order of k_F , the free-electron approximation should not be too bad in our case. The effect of introducing a finite band gap is to reduce the dielectric constant from the free electron value.

Heine and Abarenkov⁷ make further refinements on their potential which we shall not include. We are admittedly seeking an empirically determined band structure and we use the *a priori* calculation mainly as a guide to maintain reasonable contact with reality.

We adapt the Heine-Abarenkov potential, $V_{\text{HA}}(\mathbf{k}, \mathbf{k}')$ to experiment by introducing factors $F(K)$ which depend only on the momentum transfer.

$$V_F(r, r') = \sum_{\mathbf{k}, \mathbf{K}} V_F(\mathbf{k}, \mathbf{k}') \cos(\mathbf{K} \cdot \boldsymbol{\tau}/2) e^{i\mathbf{k} \cdot r} e^{-i\mathbf{k}' \cdot r'}, \quad (5)$$

$$V_F(\mathbf{k}, \mathbf{k}') = F(K) V_{\text{HA}}(\mathbf{k}, \mathbf{k}').$$

We further set the structure factor $\cos(\mathbf{K} \cdot \boldsymbol{\tau}/2)$ equal to unity for the "forbidden" K vector, $(2\pi/a)(2,2,2)$. The vanishing of this term is a consequence of superimposing identical atomic potentials, but is not required by group theory. We expect that if the Heine-Abarenkov approach is a good one, $F(2,2,2)$ will be close to zero while the other $F(K)$ will be near unity.

A. Effect of Exchange

In our calculations we have not made any allowance for the effect of exchange except for making the "Hubbard correction" to the Lindhard dielectric constant. Of course, the use of the experimentally determined factors $F(K)$ will include exchange as well as any other effects that have been left out or miscalculated. Exchange¹³ is well known to be an important effect in calculations of the cohesive energy. The first-order perturbation treatment of exchange for free electrons shows a rather strong k dependence of the exchange energy¹³ which would be expected to produce important contributions to the shape of energy bands. However, the use of screened exchange greatly reduces the k dependence.

¹¹ J. Lindhard, Kgl. Danske Videnskab. Selskab, Mat. Fys. Medd. 28, No. 8 (1954); H. Ehrenreich and M. H. Cohen, Phys. Rev. 115, 786 (1959); S. L. Adler, *ibid.* 130, 1654 (1963).

¹² D. R. Penn, Phys. Rev. 128, 2093 (1962).

¹³ F. Seitz, *Modern Theory of Solids* (McGraw-Hill Book Company, Inc., New York, 1940), p. 365.

TABLE III. Sensitivity of band-structure constants to variation of the Fourier coefficients of the potential. Tabulated numbers are $\partial A/\partial F(K)$ except for the last column which is $\sum_K \partial A/\partial F(K)$; $K^2 \geq (2\pi/a)^2 19$. Tabulated values are computed for the values of $F(K)$ given in Table II.

$\backslash K$ A	$2\pi/a(1,1,1)$	$2\pi/a(2,2,0)$	$2\pi/a(3,1,1)$	$2\pi/a(2,2,2)$	$2\pi/a(4,0,0)$	$K^2 \geq (2\pi/a)^2 19$
$(2m/\hbar^2)G'$	-0.04	-0.02	0.06	-0.25	0.03	-0.10
$(2m/\hbar^2)H'$	3.7	-0.80	2.5	-4.3	1.0	-0.37
$(2m/\hbar^2)F'$	0.22	3.7	6.5	-5.5	1.4	-1.0
m_0/m_{11}	-0.14	0.017	0.14	-0.011	0.12	-0.04
m_0/m_1	-3.7	-0.40	-1.7	1.2	-0.57	-0.17
E_G in eV	4.3	0.32	2.3	-2.2	0.63	-0.30

Quinn and Ferrell⁸ have calculated the exchange self-energy of a free-electron gas using ω and k -dependent dielectric screening of the exchange. We have evaluated their formulas for an electron density appropriate to silicon and have found that the real part of the self-energy is independent of k to within 0.03 eV in the energy range from the Fermi level E_F to $E_F + 7.0$ eV. The effect of exchange may be thought of rather accurately as rigid lowering of the free-electron energy bands without very much change in their shape. We assume that a similar rigid band shift will be the major effect of exchange in a solid as well.

III. METHOD OF CALCULATION

We have followed the procedure used by Brust¹⁴ to compute energy bands from the crystal pseudopotential; namely, we have treated exactly all interactions between plane waves of kinetic energy less than 35 eV and have used Löwdin perturbation theory¹⁵ to second order to include interactions with plane waves of kinetic energy between 35 and 90 eV. In the Löwdin method, the total interaction, h_{ij}^{tot} , between two plane waves i, j of energy less than 35 eV, consists of the direct interaction, h_{ij} , as computed from the potential, plus a second-order perturbation correction due to states, J , of kinetic energy between 35 and 90 eV:

$$h_{ij}^{\text{tot}} = h_{ij} + \sum_J \frac{h_{iJ}h_{Jj}}{[(E_i + E_j)/2] - E_J}. \quad (6)$$

The E_i are the kinetic energies. Brust¹⁷ has made a careful study of the convergence of the energy computed by this method and finds changes as large as 0.1 eV as the 90 eV bound is increased. We take this figure as an estimate of the limit of computational accuracy of our results. This figure could be improved with the use of more computer time, but we suspect that errors at least as great and possibly greater are inherent in the model which we use. We have no reliable way of estimating the errors due to approximations in the model.

The effective Hamiltonian of Eq. (6) is k -dependent

for two reasons. First, h_{ij} is k -dependent because of the angular-momentum dependence of the potential. Second, the perturbation term in Eq. (6) gives a k dependence through the kinetic energy in the denominator. In computations of the effective mass, both of these sources of k dependence must be included in addition to the simple " $\mathbf{k} \cdot \mathbf{p}$ effect"¹⁸ from the kinetic energy of states below 35 eV. Table II demonstrates a rather weak k -dependence of the direct interaction, h_{ij} . We had accordingly supposed that most of the effective mass would be accounted for by the simple $k \cdot p$ effect. Actual calculations showed that both sources of k dependence made comparable contributions to the mass, their sum amounting to as much as 20% of the total.

IV. EMPIRICAL ADJUSTMENT OF THE MODEL POTENTIAL

In adapting the Heine-Abarenkov potential⁷ to experiment with the factors $F(K)$ of Eq. (5), we have considered six experimentally determined constants to be reliably and accurately established; namely, the indirect gap, $E_G = 1.15$ eV,¹⁹ the conduction-band masses, $m_{11}^{-1} = 1.09 m_0^{-1}$, and $m_{11}^{-1} = 5.25 m_0^{-1}$,²⁰ and the valence-band mass constants, $L = -6.76 (\hbar^2/2m)$, $M = -4.51 (\hbar^2/2m)$, $N = -9.35 \hbar^2/2m$.²¹ (m_{11} and m_1 are parallel and perpendicular to the $[100]$ direction, respectively.) Instead of using L, M, N directly we prefer to work with the constants F, G, H_1, H_2 defined by Dresselhaus *et al.*²² F arises from " $k \cdot p$ interaction" of the Γ_{25} valence band with states of $\Gamma_{2'}$ symmetry, G comes from $\Gamma_{12'}$ symmetry, H_1 from Γ_{15} symmetry, and H_2 from Γ_{25} symmetry. H_2 is expected to be very small. Instead of assuming $H_2 = 0$, we define the quantities

$$\begin{aligned} G' &= G + \frac{2}{3}H_2, \\ H' &= H_1 + H_2, \\ F' &= F - \frac{4}{3}H_2. \end{aligned} \quad (7)$$

¹⁸ E. O. Kane, J. Phys. Chem. Solids **1**, 83 (1956).

¹⁹ A. Frova and P. Handler, Phys. Rev. Letters **14**, 178 (1965).

²⁰ J. C. Hensel, H. Hasegawa, and M. Nakayama, Phys. Rev. **138**, A225 (1965).

²¹ J. C. Hensel and G. Feher, Phys. Rev. **129**, 1041 (1963).

²² G. Dresselhaus, A. F. Kip, and C. Kittel, Phys. Rev. **98**, 368 (1955).

¹⁴ D. Brust, Phys. Rev. **134**, A1337 (1964).

¹⁵ P. Löwdin, J. Chem. Phys. **19**, 1396 (1951).

¹⁶ Reference 13, p. 340.

¹⁷ D. Brust, Phys. Rev. **139**, A489 (1965).

TABLE IV. Band-structure constants used to determine the pseudopotential, $V_F(\mathbf{k}, \mathbf{k}')$ for silicon. The experimental constants are determined from the valence-band and conduction-band cyclotron-resonance constants and the indirect energy gap E_G .

	Experimental	Computed
$2m/\hbar^2 G'$	-0.64	-1.00
$2m/\hbar^2 H'$	-4.51	-4.48
$2m/\hbar^2 F'$	-5.48	-5.68
m_0/m_{11}	1.09	1.09
m_0/m_{\perp}	5.25	5.06
E_G in eV	1.15	1.01

Using Dresselhaus *et al.*,²² we then have

$$\begin{aligned} F' &= (L + 2N - 2M)/3, \\ H' &= M, \\ G' &= (L - N + M)/3. \end{aligned} \tag{8}$$

To adjust the band structure to fit these six experimental quantities we have chosen to vary the coefficients $F(K)$ of the five principal plane waves of lowest kinetic energy. As a sixth parameter we vary the coefficients $F(K)$ for all principal plane waves greater than the five lowest, using a single constant independent of K for all $K^2 \geq (2\pi/a)^2 19$.

We computed a 6×6 matrix, shown in Table III, which gives the derivatives of the experimental quantities which we wish to fit with respect to the six theoretical parameters. We assume that changes in the experimental quantities are linear in the theoretical parameters and use Table III to correct the $F(K)$ from the initial values $F(K) = 1, K \neq (2\pi/a)(2, 2, 2); F(K) = 0, K = (2\pi/a)(2, 2, 2)$ to give the right values of the experimental numbers. Since the assumption of linearity is not exact, we had to iterate the above procedure several times. We also recomputed the matrix of Table III for the final values of $F(K)$. The final values of F are given in Table II together with the final potential coefficients $V_F(\mathbf{k}, \mathbf{k}')$ which give the best fit to experiment. The computed values of the experimental quantities are given in Table IV.

In the course of the calculations it became clear that the 6 parameters were not as independent as would be desired. In order to study this point we constructed the orthonormality matrices of Table V. In the first two parts of Table V we treat the rows of the 6×6 matrix in Table III as vectors and compute the "lengths" of these vectors as well as the "dot products" of the normalized vectors, $W_{\text{row } j} \cdot W_{\text{row } k} / (|W_{\text{row } j}| |W_{\text{row } k}|)$. Clearly, a "dot product" equal to zero means the parameters are completely independent whereas a "dot product" of one means complete dependence. The row "lengths" indicate the sensitivity of the experimental parameter labeling the row to the variation of the potential. It is clear that the experimental parameters G' and m_0/m_{11} are 20 to 30 times less sensitive to the potential than the other parameters. We note also from Table V that the quantities $m_0/m_{\perp}, E_G$, and H'

TABLE V. Orthogonality of experimental and theoretical parameters in Table III. The rows in Table III are treated as "experimental" vectors W_j^E , where the subscript j refers to an experimental quantity. The columns are considered "theoretical" vectors W_j^T , where the subscript refers to the potential coefficient for a given plane wave. The first two parts give the "lengths" and normalized "dot products" $W_j^E \cdot W_k^E / (|W_j^E| |W_k^E|)$ for the "experimental" row vectors, while the last two parts give the same information for the theoretical column vectors.

"Experimental" vector lengths						
j	G'	H'	F'	m_0/m_{11}	m_0/m_{\perp}	E_G
W_j^E	0.28	6.3	9.4	0.24	4.3	5.4
Vector orthonormality; $W_j^E \cdot W_k^E / W_j^E W_k^E $						
$j \backslash k$	G'	H'	F'	m_0/m_{11}	m_0/m_{\perp}	E_G
G'	1	0.65	0.69	0.36	-0.20	0.37
H'		1	0.66	0.00	-0.85	0.92
F'			1	0.54	-0.51	0.59
m_0/m_{11}				1	0.20	-0.13
m_0/m_{\perp}					1	-0.98
E_G						1
Theoretical pseudopotential vectors						
j	(1,1,1)	(2,2,0)	(3,1,1)	(2,2,2)	(4,0,0)	$K^2 \geq 19$
W_j^T	6.8	3.8	7.5	7.4	1.9	1.1
Vector orthonormality $W_j^T \cdot W_k^T / (W_j^T W_k^T)$						
$j \backslash k$	(1,1,1)	(2,2,0)	(3,1,1)	(2,2,2)	(4,0,0)	$K^2 \geq 19$
(1,1,1)	1	0.027	0.53	-0.62	0.68	-0.29
(2,2,0)		1	0.81	-0.64	0.66	-0.80
(3,1,1)			1	-0.96	0.97	-0.92
(2,2,2)				1	-0.99	0.91
(4,0,0)					1	-0.86
$K^2 \geq 19$						1

are closely correlated, the correlation between m_0/m_{\perp} and E_G being especially strong. As a consequence of these relationships, we may say, loosely speaking, that we have between 2 and 3 truly independent parameters.

In the last two parts of Table V we treat the columns of Table III as vectors and compute their lengths and normalized "dot products." The "lengths" in this case demonstrate the relative effectiveness of the different potential coefficients in changing the band structure. The magnitude of the (222) coefficient may be somewhat misleading. According to our choice of definitions, the change of an "allowed" coefficient from 1 to 1.1 say, is put on an equal footing with a change of the "forbidden" coefficient from 0 to 0.1. The latter change is probably less likely than the former, so that the V_{222}^T sensitivity in Table V is probably too large. [Note that in diamond the x-ray scattering from the 222 component of charge density is about 10% of that from allowed components,²³ whereas our values of $F(K)$ are around 30% different from the theoretical values.]

The dependence of parameters found in the first two parts of Table V must necessarily also appear in the

²³ L. Kleinman and J. C. Phillips, Phys. Rev. **125**, 819 (1962).

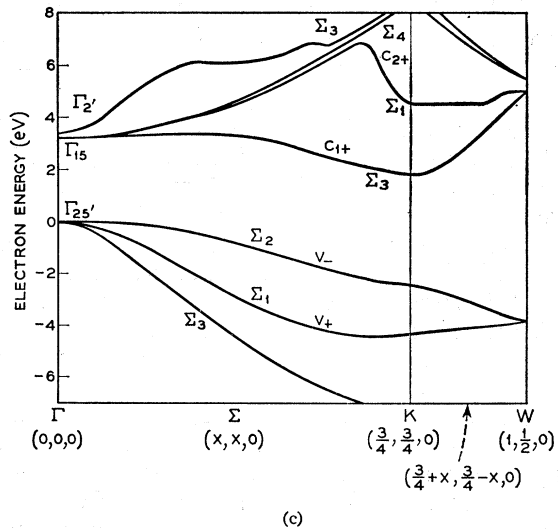
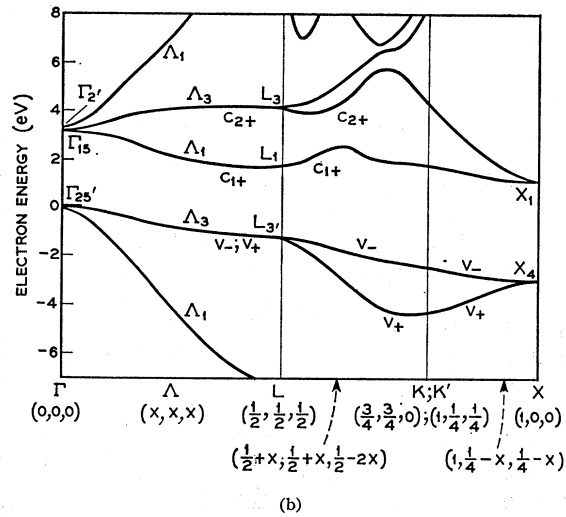
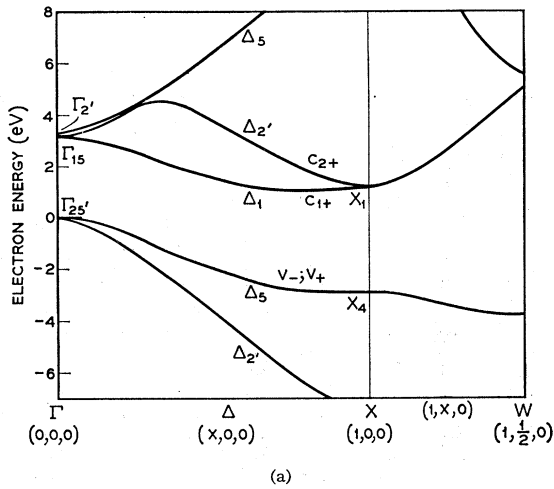


FIG. 1. Energy bands of silicon as computed by the Heine-Abarenkov method modified to fit experiment. The c_{\pm}, v_{\pm} labels identify the bands involved in the "optical energy" contours of Fig. 3.

last two parts. We see that, in fact, the four highest plane waves in the table produce nearly equivalent effects.

As shown in Table IV we have not achieved a perfect match to the 6 experimental quantities with our 6 theoretical parameters. This is due to the lack of independence noted above and the fact that we restricted the range of $F(K)$ to "reasonable" values; $0.5 < F(K) < 2$, $K \neq (2\pi/a)(2,2,2)$ and $|F((2\pi/a)(2,2,2))| < 0.2$. Concomitant with this lack of perfect matching is a considerable ambiguity in the values of $F(K)$ which give an adequate fit with experiment. The values listed in Table II are by no means unique, they are merely a possible set of parameters. We believe the band structure is much more nearly unique than the pseudopotential.

The largest discrepancy between experimental and computed parameters is the 0.36 ($\hbar^2/2m$) error in the parameter G' . The general good agreement of all experimental parameters in spite of their lack of inde-

pendence gives confidence in the general validity of the approach.

V. RESULTS OF CALCULATION

The results of the present calculation of the band structure of silicon are presented in Fig. 1. Comparison is made in Table VI between the present calculation

TABLE VI. Comparison of principal energy gaps between present calculation and that of Brust.^a

Gap	Energy in eV	
	Brust ^a	This work
$\Gamma_{25'} - \Gamma_{2'}$	3.8	3.3
$\Gamma_{25'} - \Gamma_{15}$	3.4	3.2
$L_3' - L_1$	3.1	2.9
$L_3' - L_3$	5.4	5.3
$X_4 - X_1$	4.0	4.1

^a Reference 14.

TABLE VII. Distribution in k space of the contributions to $\epsilon_2(\omega)$. $k = (2\pi/a)(n_1/4, n_2/4, n_3/4)$.

	Cubic Mesh Point																			
	n_1	n_2	n_3	3.4	3.5	3.6	3.7	3.8	3.9	4.0	4.1	4.2	4.3	4.4	4.5	4.6	5.2	5.3	5.4	5.5
Γ	0	0	0	1.7	0.89	0.93	0.42	0.27	0.14	0.07	0.06	0.07	0.01	0.04	0.05	0.03	0.00	0.00	0.00	0.00
Δ	1	0	0	3.7	2.5	1.9	2.2	2.4	1.5	1.0	0.80	0.42	0.64	0.59	0.33	0.65	0.42	0.46	0.39	0.48
Σ	1	1	0	3.1	4.4	4.1	3.9	4.1	3.8	4.7	3.2	2.5	2.7	2.3	1.8	1.8	0.65	0.41	0.44	0.36
Λ	1	1	1	2.6	3.3	2.3	1.7	0.97	1.1	0.57	0.67	0.45	0.78	1.1	0.82	0.99	1.1	1.2	1.0	0.76
Δ	2	0	0	0.89	2.9	5.7	2.8	2.3	1.3	0.93	0.22	0.11	0.05	0.01	0.00	0.00	0.00	0.04	0.48	0.57
	2	1	0	0.00	0.00	0.33	1.2	1.7	3.5	3.9	3.6	4.0	3.0	2.4	2.1	2.2	1.4	1.4	1.3	1.1
	2	1	1	2.3	1.7	3.5	3.0	2.5	3.4	3.1	4.5	5.5	8.6	3.9	2.6	1.5	2.1	1.9	2.4	1.9
Σ	2	2	0	0.00	0.00	0.00	0.00	0.00	0.08	0.38	1.0	2.9	6.0	3.8	2.1	1.3	0.32	0.32	0.42	0.50
	2	2	1	2.2	3.0	2.9	3.0	2.7	3.8	5.1	4.1	6.7	6.0	3.6	2.1	2.0	0.60	2.8	4.1	1.7
L	2	2	2	1.9	1.1	1.4	0.89	0.73	0.16	0.23	0.11	0.12	0.03	0.04	0.00	0.01	0.02	1.1	1.4	0.98
Δ	3	0	0	0.00	0.00	0.66	1.3	3.0	3.5	4.0	2.7	0.97	0.55	0.27	0.58	0.56	0.72	0.89	0.72	0.32
	3	1	0	0.00	0.00	0.00	0.00	0.00	0.00	0.57	1.9	3.2	2.8	2.4	2.7	2.0	1.7	1.4	1.4	1.6
	3	1	1	0.00	0.00	0.00	0.00	0.00	0.00	0.00	0.21	5.8	11	6.7	4.1	3.9	0.34	0.30	0.21	0.19
	3	2	0	0.00	0.00	0.00	0.00	0.00	0.00	0.00	0.00	0.00	1.7	1.3	1.1	0.62	0.63	1.1	0.67	0.69
	3	2	1	0.00	0.00	0.00	0.00	0.00	0.00	0.00	0.20	0.51	2.7	3.0	3.1	2.1	1.6	2.0	1.6	1.5
K	3	3	0	0.00	0.00	0.00	0.00	0.00	0.00	0.00	0.52	6.0	5.5	3.0	2.1	1.6	0.22	0.18	0.10	0.11
X	4	0	0	0.00	0.00	0.00	0.00	0.00	0.10	1.3	2.1	2.3	0.70	1.2	0.64	0.42	0.05	0.05	0.02	0.02
	4	1	0	0.00	0.00	0.00	0.00	0.00	0.00	0.00	0.15	1.3	1.4	1.1	1.2	1.2	0.90	1.0	0.76	0.96
W	4	2	0	0.00	0.00	0.00	0.00	0.00	0.00	0.00	0.00	0.00	0.00	0.00	0.00	0.00	0.00	0.00	0.00	0.00
Total	ϵ_2	18	20	24	21	21	22	26	26	44	55	37	27	23	12.8	16.7	17.5	13.7		

and the pseudopotential calculation of Brust,¹⁴ based on the BCP parameters.⁵ The differences are generally of the order of 0.1 to 0.2 eV, which is probably the limit of over-all accuracy of either calculation. For the $\Gamma_{25'} - \Gamma_{2'}$ gap, the discrepancy is larger, 0.5 eV, or about 15%. We indicate a mild preference for our value here, since it is more closely related to an experimental number than is the BCP⁵ band structure.

BCP⁵ used only three parameters to obtain their band structure, whereas we have used six. We are not surprised, *a posteriori*, at the close agreement between us since we have found that our parameters were not really independent. The close agreement is more surprising because BCP determined their potential on the basis of the energy gaps Γ , X , and L inferred from optical data, whereas we have used the indirect gap and cyclotron masses. Offhand, this result appears to suggest that the structure in ϵ_2 , the imaginary part of the dielectric constant, is indeed due to critical points located at these high symmetry points. We have found that this is not strictly true, as we shall detail later. What appears to be more nearly true is that the energy gaps at Γ , X , and L are very close in energy to the energies of the prominent structure in ϵ_2 with which they have been identified. From the point of view of determining band structure this weaker statement is, of course, all that is necessary.

We have computed the energy bands of silicon on a simple cubic mesh with spacing $\Delta k_x = \Delta k_y = \Delta k_z = (2\pi/a)(1/8)$. The model potential interactions between plane waves of kinetic energy less than 35 eV were treated exactly, whereas the interactions with states having kinetic energy between 35 and 90 eV were treated by Löwdin perturbation theory as mentioned earlier. States were grouped together into quasi-

degenerate multiplets if the energy separation of a given level with the level nearest in energy was less than 1 eV. With this choice, the maximum number of elements in any multiplet was 5. Energy matrix elements for any value of k between members of a given multiplet may be calculated correct to order $(\Delta k)^2$ by eliminating " $\Delta k \cdot p$ " interactions^{15,18} connecting multiplet states with states outside the multiplet to this order. The energy matrix element, M_{ij} , between multiplet members i and j may then be written

$$M_{ij} = \epsilon_i \delta_{ij} + \sum_{m=1}^3 P_{ijm} \Delta k_m + \sum_{m, n=1}^3 R_{ijmn} \Delta k_m \Delta k_n, \quad (9)$$

where $\Delta \mathbf{k} = \mathbf{k} - \mathbf{k}_{\text{mesh}}$. The ϵ_i are the energies computed at the mesh points. The P_{ijm} and R_{ijmn} were also computed in order to extrapolate the energy to k values other than mesh points. This is, of course, done by computing M_{ij} for the appropriate value of $\Delta \mathbf{k}$ and diagonalizing the multiplet matrix, M_{ij} .

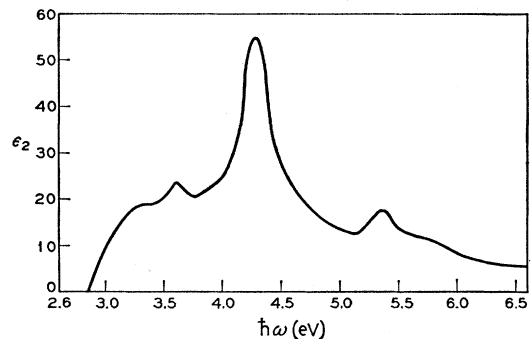


FIG. 2. The imaginary part of the dielectric constant, $\epsilon_2(\hbar\omega)$, as computed by a Monte Carlo method with the band structure of the present paper.

We remarked before that the simple “ $k \cdot p$ ” calculation¹⁸ which ignores the k dependence of the model Hamiltonian (except for the diagonal kinetic energy) gave errors of the order of 20% in computing masses. Unfortunately, the exact calculation is not diagonal in the plane-wave basis states as is the “simple $k \cdot p$ ” contribution. This fact results in a great increase in computing time. We made the compromise of treating the k dependence of the Hamiltonian, but only computing that part of the contribution which was diagonal in k . This procedure reduced the mass errors from 20% to $\sim 10\%$ for the worst case tested.

VI. CALCULATION OF $\epsilon_2(\omega)$

We have used our band structure to compute the imaginary part of the dielectric constant, ϵ_2 , using the formula¹⁴

$$\epsilon_2(\omega) = \frac{e^2}{3\pi m_0^2 \omega^2} \sum_{i,j} \int_{\text{B.Z.}} d\mathbf{k} |\mathbf{p}_{ij}(\mathbf{k})|^2 \delta(E_i(\mathbf{k}) - E_j(\mathbf{k}) - \hbar\omega). \quad (10)$$

The summation is over empty conduction-band states i and filled valence-band states j . \mathbf{p}_{ij} is the momentum matrix element between states i and j .

The integration over the Brillouin zone (B.Z.) was performed by a Monte Carlo method.¹⁷ The upper two valence bands and the lowest four conduction bands were summed over. The matrix element p was computed rather than being taken constant.

The results of the calculation are shown in Fig. 2. Pronounced structure at 4.3 and 5.35 eV corresponds well in energy with the experimentally determined structure in ϵ_2 .²⁴ The strong peak seen in the experimental data near 3.4 eV is very weak in our computation.

Recent calculations by Brust¹⁷ show the 3.5-eV peak more prominently, though it is not as strong as the experimental peak. He has attributed this peak to transitions along Δ in agreement with the experimental results of Gerhardt.²⁵ The weaker structure that we find also appears to come from the direction Δ .

We have attempted to answer the important question of what parts of the zone make the major contributions to the critical point structure seen in ϵ_2 . Our approach is to divide the entire zone up into cubic boxes of length $(0.25)(2\pi/a)$ centered on the simple cubic mesh $(l,m,n)(2\pi/4a)$, where l,m,n are integers from zero to 4. In this way there are 19 inequivalent boxes within the “cubic sector,” $2\pi/a \geq k_x \geq k_y \geq k_z \geq 0$; $k_x + k_y + k_z \leq \frac{3}{2}(2\pi/a)$. There are, of course, 48 equivalent cubic sectors in the Brillouin zone. We count only that fraction of a “box” which lies within the cubic sector. The

²⁴ H. R. Philipp and H. Ehrenreich, Phys. Rev. **129**, 1550 (1963).

²⁵ U. Gerhardt, Phys. Letters **9**, 117 (1964); Phys. Rev. Letters **15**, 401 (1965).

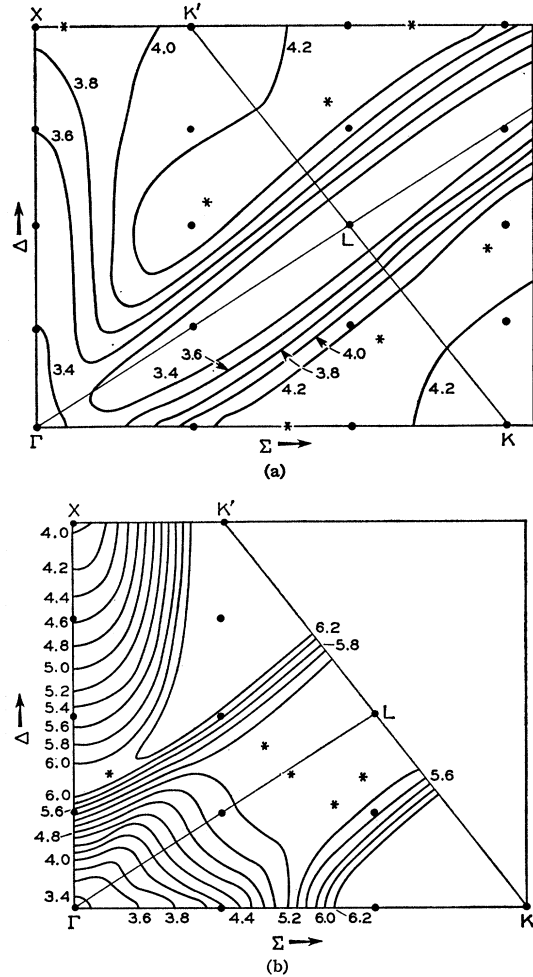


FIG. 3. Optical energy contours in the (110) plane for the band structure of Brust, Cohen, and Phillips. The contours are given by the equation $\hbar\omega = E_c(\mathbf{k}) - E_v(\mathbf{k})$. The values of $\hbar\omega$ in eV are indicated near the contour. Solid circles denote the cubic mesh points $(l,m,n)\pi/2a$. Stars identify “optical” critical points. (a)— $c=c_{1+}$, $v=v_-$. (b)— $c=c_{2+}$, $v=v_-$. In (a) the energy contours have been extended beyond the line KLK' bounding the first zone.

contribution of each box to ϵ_2 is listed in Table VII. The sum of all 19 boxes gives the total ϵ_2 as plotted in Fig. 2. The computations represent averages over a 0.1-eV energy interval. The rms statistical fluctuation is estimated to be about 5%.

It is immediately evident from the table that the structure in ϵ_2 is by no means describable by contributions from Γ , X , and L in spite of the large size of the “boxes” we have chosen. The boxes are, in fact, so large that the electron energy may vary by several electron volts or more within a single box. The boxes are centered on cubic mesh points; hence their centers lie on the important symmetry points Γ, X, L, W ; on the symmetry lines Λ, Δ , and Σ ; and in the (110) and (100) symmetry planes. Because of the large mesh size, 13 mesh points lie in the $(1\bar{1}0)$ or $(01\bar{1})$ plane, 13 lie in the (001)

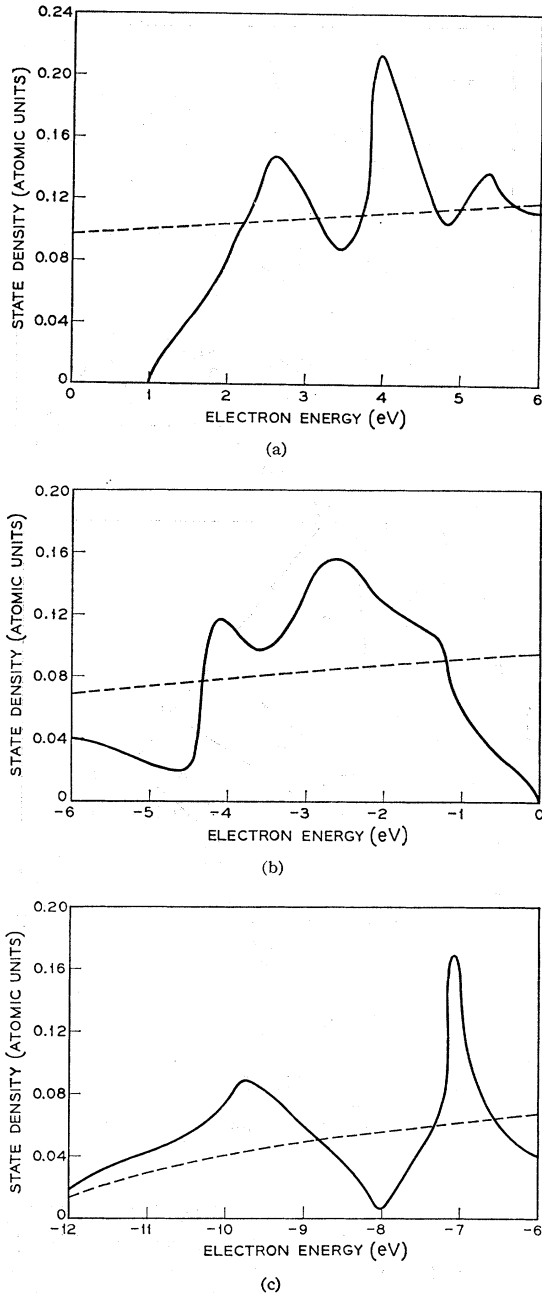


FIG. 4. Electron density of states in atomic units versus energy as calculated with the band structure of this paper. The dashed line is the free-electron density of states with an energy zero at -12.25 eV, the bottom of the valence band.

plane, and there is one "general point" $(3,2,1)\pi/2a$ which, however, lies on the $(1,1,1)(\pi/a)$ zone face.

The 4.3-eV peak, in keeping with its large size, has major contributions from a large number of mesh boxes. The 5 largest are $(3,1,1)\pi/2a$, $(2,1,1)\pi/2a$, $(2,2,0)\pi/2a$, $(2,2,1)\pi/2a$, and $(3,3,0)\pi/2a$ arranged in order of decreasing importance. These 5 boxes contribute 67% of the value of ϵ_2 at 4.3 eV. The only common feature they

have is that they lie in the $(1\bar{1}0)$ or $(01\bar{1})$ plane. The mesh box centered on X has a peak contribution at 4.2 eV which amounts to only 5% of the total value of ϵ_2 at this energy.

The contributions to the peak at 5.4 eV are a little less easy to determine because the "background" is much more important here. For instance, $(3,1,0)\pi/2a$ and $(3,2,1)\pi/2a$ make a large contribution, but because of their energy independence, they should be considered "background." Statistical fluctuations from the Monte Carlo method make the true energy dependence somewhat uncertain but $(2,2,1)\pi/2a$ and $(2,2,2)\pi/2a$ appear to be the major contributors. The "L" box is more important here than was the "X" box at 4.3 eV, but it is still less than 25% of the total peak height above background, whereas $(2,2,1)\pi/2a$ contributes about 70%.

Our calculations are less useful in studying the 3.5-eV peak. Since our computed peak is so much weaker than the experimental peak we are not sure that the distribution in k space which we find is at all representative of the true distribution. We find the maximum contribution at 3.6 eV to be from $(2,0,0)\pi/2a$ in agreement with Gerhardt's experimental determination²⁵ that the 3.5-eV critical point has Δ symmetry. Brust's¹⁷ calculations also suggest a strong contribution to ϵ_2 from this region.

We have also studied the k distribution of ϵ_2 by the energy contour method. These calculations were made prior to the present study and used the three-parameter band structure of Brust, Cohen, and Phillips.⁵ As we have already noted, the differences with the present band calculations are very slight.

The important mesh points responsible for critical point structure in ϵ_2 have been found to lie in the (110) plane. In Fig. 3 we have plotted "optical-energy contours" in the (110) plane; i.e., we plot $\hbar\omega = E_c(\mathbf{k}) - E_v(\mathbf{k})$ for \mathbf{k} in the (110) plane with fixed photon energies, $\hbar\omega$.

Since reflection in the (110) plane is a symmetry operation for k in the (110) plane, the energy bands can be characterized by + or - "reflection parity." The use of "reflection parity" avoids discontinuities introduced by the energy-ordering definition of bands and simplifies the computation of energy contours. The contours plotted are for the odd-parity valence band, v_- , (there is only one) to the lowest and next lowest even-parity conduction bands, designated c_{1+} and c_{2+} , respectively. These bands are identified in Fig. 1.

In Fig. 3(a) we have extended the energy contours beyond the line $K'LK$ which bounds the first zone in order to show that the "flat" region of the optical energy bands is really one continuous piece rather than two separate sections. The mesh points are indicated in the figure as solid circles. Critical points are tentatively identified by stars. Because of the extreme flatness of the surface the identification of critical points is not accurate, hence we cannot be sure of their location or even their number.

TABLE VIII. Sensitivity to potential variation of the gap between bands 4 and 5 at different points in k space.

k in units of ($2\pi/a$)	$\Delta E = E_5(k) - E_4(k)$ in eV	$d(\Delta E)/dF(K)$ in eV		
		$K = (2\pi/a)$ (1,1,1)	$K = (2\pi/a)$ (2,2,0)	$K = (2\pi/a)$ (3,1,1)
(0.6,0.6,0)	4.24	2.86	0.38	1.88
(0.65,0.27,0.27)	4.31	2.42	0.41	1.67
(1,0,0)	4.08	2.94	0.48	1.54
(0.625,0,0)	3.56	2.55	0.45	1.67
(0.375,0,0)	3.31	2.33	0.22	1.70
(0,0,0)	3.15	2.52	-0.38	2.00
(0.5,0.5,0.5)	2.83	1.53	1.10	2.46

The 5 mesh points which contribute most to the 4.3-eV peak are seen to lie in the very flat, triangularly shaped region in the upper part of the figure. The "X" point is on the extreme edge of this triangular region.

The flatness along the Δ direction at 3.5 eV is seen in Fig. 3(a) as Brust¹⁷ has already noted.

In Fig. 3(b) the 5.4-eV peak in ϵ_2 is associated with a squarish region about the "L" point. It appears that further critical points near "L" are required to make a large enough flat region to show up as a prominent peak in ϵ_2 .

Inasmuch as strong peaks seem to require large flat regions in k space, it is interesting to inquire whether these regions are "stable" against small variations of the potential. In Table VIII we show the derivatives of the optical energy separations with respect to $F(K)$ for the three lowest K values computed for a number of different k points in the (110) plane.

The first three rows refer to points in the "flat" region of Fig. 3(a). The coefficients vary by no more than 20% over this region, hence we expect to be able to shift the 4.3-eV peak as a whole by changing the potential without drastically reducing its strength or broadening it. These coefficients also show that the "X" point energy difference moves along with the 4.3-eV peak even though it contributes only weakly to its strength.

The coefficients along the entire Δ line are also fairly constant except for the $(2\pi/a)(2,2,0)$ coefficient which is relatively small. If the 3.5-eV peak comes from the Δ direction, it will also be relatively stable against potential variations.

For comparison, we note that the coefficients at the L point are quite different from the other entries in the table.

VII. ELECTRONIC DENSITY OF STATES

In Fig. 4 we give the results of a computation of the electronic density of states in atomic units using our band structure. We computed the density of states from the formula

$$\rho(E) = \frac{2V}{(2\pi)^3} \sum_i \int_{\text{B.Z.}} dk \delta(E_i(\mathbf{k}) - E). \quad (11)$$

We performed these calculations by a Monte Carlo method in the same way as we calculated ϵ_2 . The lowest 8 energy bands were summed over.

For comparison the free-electron density of states is shown as a dashed line. The bottom of the valence band at -12.25 eV is taken as the energy zero in the free-electron calculation.

Our results are in good agreement with calculations by Brust.¹⁷ He summed only over bands 4, 5, and 6 so that our results are valid over a larger energy range, namely from -12 to +6 eV. (We follow Brust's convention of labeling the bands in order of increasing energy.)

The 4.0-eV peak appears to be quite important in photoemission studies.^{17,26} The other structure has not yet been identified experimentally. The sharp peak at -7 eV and the strong dip at -8 eV are outstanding features.

²⁶ F. G. Allen and G. W. Gobeli (to be published).